OBSERVATION OF HF NOISE IN AN INTENSE AURORA BY THE SOUNDING ROCKET S-310JA-7

Yoshiharu NAKAMURA and Yuzi NOMURA

The Institute of Space and Astronautical Science, 6–1, Komaba 4-chome, Meguro-ku, Tokyo 153

Abstract: Observation of noise in the frequency range from 0.6 to 7.6 MHz has been made in an auroral plasma up to approximately 220 km by an instrument (PWN-H) on board the S-310JA-7 sounding rocket. This rocket was launched at 1915: 50 UT on March 27, 1978 from Syowa Station in Antarctica, just prior to an intense auroral substorm (magnetic H component decrease $=-700$ nT and 30 MHz CNA $=-5$ dB). The observed HF emissions are classified into three types according to their frequency ranges and spectral shape; 1) High level and narrow band signals whose frequencies are nearly equal to nf_{ce} or $(n+1/2)f_{ce}$, where n is an integer and f_{ce} is the electron gyrofrequency. 2) A low level broad band emission whose upper-limiting frequency is below the local electron plasma frequency. 3) Signals at frequencies below f_{ce}. Excitation mechanism of these waves in the aurora is discussed.

1. Introduction

In auroras, there are precipitating electrons with a few hundred eV to about ten keV in energy, which carry the field-aligned upward current and which are expected to drive instabilities causing natural plasma emissions, in the frequency range from the VLF to the HF, due to wave-particle interaction. Much attention has been given to date to waves in the VLF range because ground observations have frequently received waves in the VLF range and the auroral hiss has been studied simultaneously with auroral activity by scientific satellites.

Recently, at low altitudes in the polar ionosphere, observations of natural emissions in the MF and HF ranges have been made by using sounding rockets. Electron plasma oscillations in the Bernstein mode, which lies between the first and second harmonics of the electron cyclotron frequency f_{ce}, and whistler waves have been observed (KELLOGG *et al.*, 1978). A series of rocket experiments to investigate the characteristics of the plasma in the polar ionosphere, especially in auroras, has been performed from 1976 to 1978 at Syowa Station in Antarctica by the National Institute of Polar Research. Electron plasma waves, signals at a frequency about one half of f_{ce}, emissions whose lower cutoff frequency is the electron plasma frequency, and whistler waves whose frequencies are considerably below f_{ce} have been observed. Their correlation with observations of precipitating energetic electrons and comparisons of theoretical calculations with observational data have been performed (OYA *et al.*, 1979, 1980; MIYAOKA *et al.*, 1981).

The S-310JA-7 sounding rocket was one of the series, which was successfully

launched by the 19th Japanese Antarctic Research Expedition. A swept-frequency receiver (PWN-H) was mounted on the rocket to receive the natural emissions in the HF range. The rocket passed through an auroral arc detecting new emissions which are described in this paper. The PWN-H system is described in Section 2. The observational results are presented in Section 3 and discussed in Section 4. Section 5 is the conclusion.

2. PWN-H Instrumental System

Figure 1 shows the block diagram of the PWN-H instrument. The outer grid and the ring of a Faraday cup of 10 cm diameter, positioned on the top of the rocket, was used as a receiver antenna (ITOH *et al.*, 1975). The electron saturation current from the ambient plasma was drawn to the grid (G_1) by a bias of 3 V with respect to the rocket body. The total area of the grid including the ring was 28 cm^2. The AC component of the current carries information on the density perturbation caused mainly by electrostatic waves. The electron saturation current was amplified and was logarithmically converted to an output voltage in the range from 0 to 5 V. The AC component of the electron current was also amplified and was fed into the swept frequency double super-heterodyne receiver. The receiver covered the frequency range from 0.6 to 7.6 MHz. The output of the receiver was rectified and was loga-

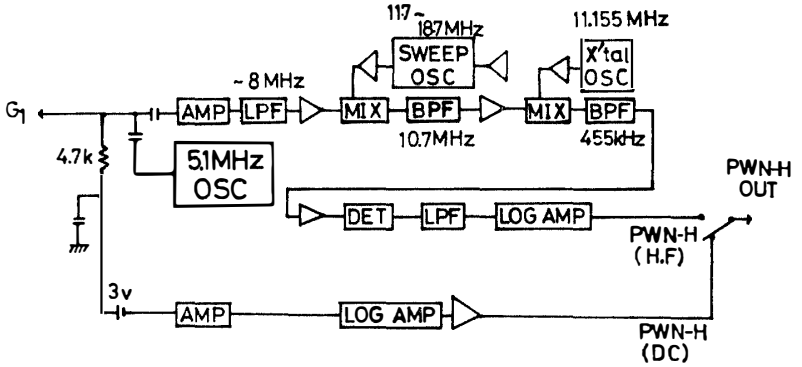

Fig. 1. Block diagram of the PWN-H instrumentation. The PWN-H consists of three principal parts: 1) G_1, the grid 1 as the antenna of the receiver. 2) The amplifier for the AC component of the current and the frequency analyzer. 3) The amplifier for the DC component.

Table 1. The specifications of PWN-H on board the rocket.

Frequency range	0.6~7.6 MHz
Sweep time	1 s
1st IF frequency	10.7 MHz
2nd IF frequency	455 kHz
Band width	30 kHz
Sensitivity	0.35~300 μV_{rms}
Sensor	10 cmϕ F.C.
Telemeter ch.	IRIG #10

rithmically converted to a voltage in the range from 0 to 5 V. A calibration signal of 5.1 MHz was continuously applied to the input. The output voltages of both DC and AC component were transmitted to a ground station alternately every second using an IRIG 10th telemeter channel. The specification of the PWN-H system are listed in Table 1.

3. The Results of the Observation

The S-310JA-7 rocket was launched at 1915:50 UT on March 27, 1978 from Syowa Station (geomagnetic latitude, 70.0°; longitude, 79.4°; L=6.1) in Antarctica into the geomagnetic north direction at an azimuth of 315° and reached an apogee of approximately 220 km. The geomagnetic activity just after the launching was very intense with an H component variation of geomagnetic field $\Delta H = -700$ nT. The cosmic noise absorption (CNA) at 30 MHz was nearly equal to −5 dB. Intense VLF hiss emissions on 8.2 and 0.75 kHz were detected at the ground.

Figure 2 shows the geomagnetic meridian plane and time diagram of OI5577Å

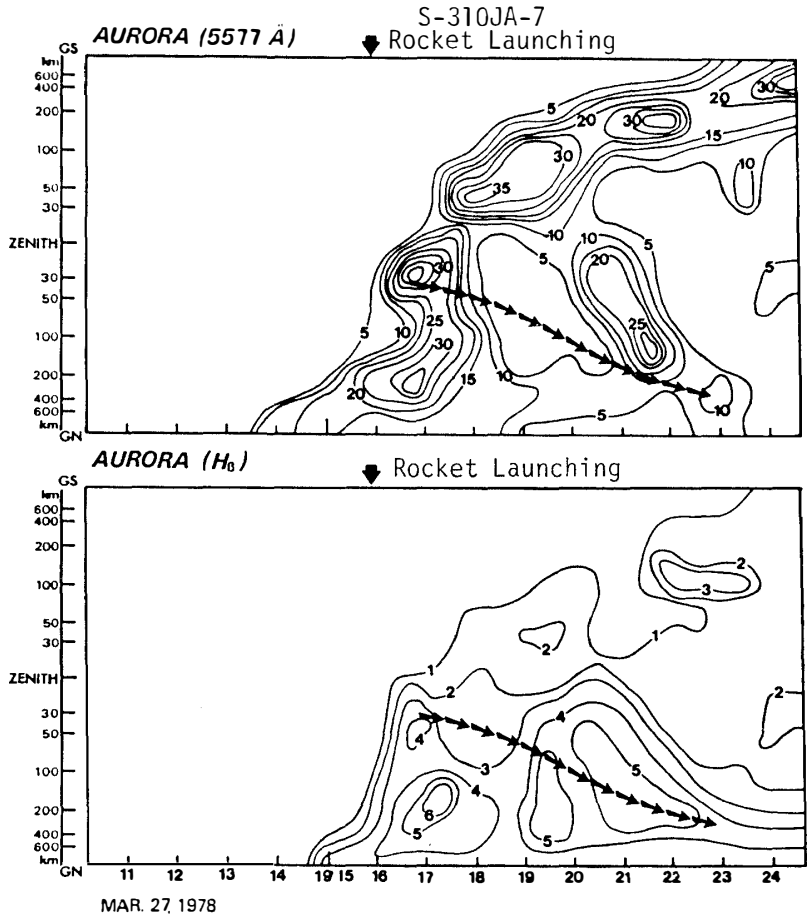

Fig. 2. The meridian-time diagram of intensities of OI5577Å and H_β (after HIRASAWA and YAMAGISHI, 1980). The contours of the auroral luminosity is units of 1 kR for 5577Å and 100R for the H_β line. The rocket trajectory indicated by the arrow is projected onto the 100 km level along geomagnetic field lines.

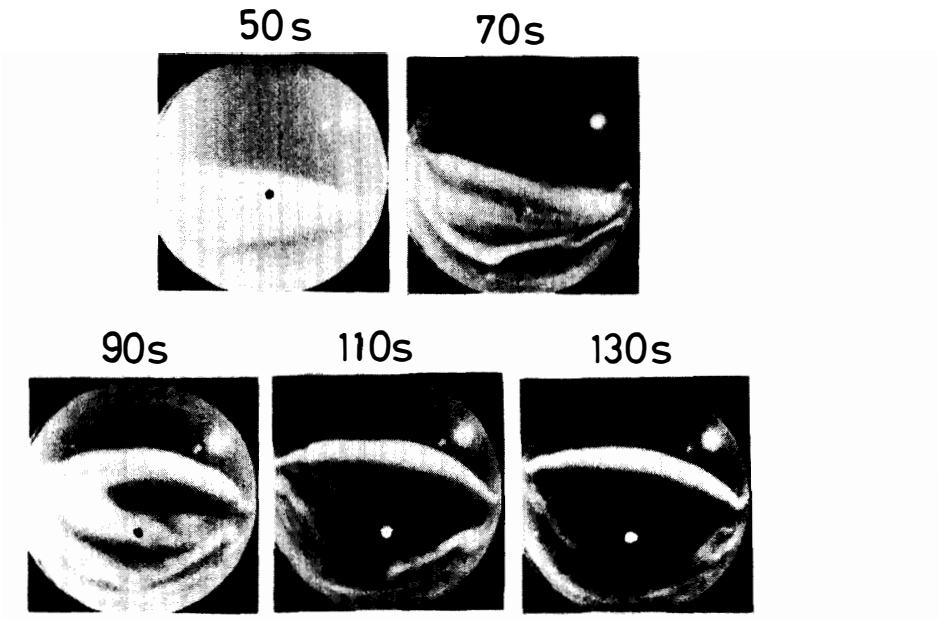

Fig. 3. All-sky photographs of the aurora taken at Syowa Station at several times after the rocket launching. The top is magnetic South and the bottom is magnetic North direction. Positions of the rocket are projected to the 100 km level along magnetic field lines.

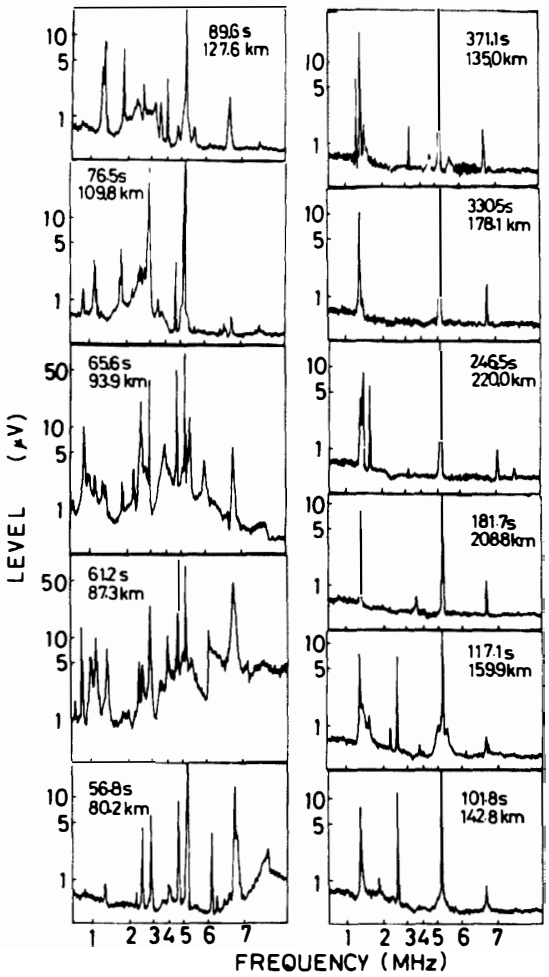

Fig. 4. Typical raw data of received noise in the HF range. The panels on the left side show the noise observed in the intense aurora. The right side panels show the observed noise after the rocket passed through it. The narrow peaks at 5.1 MHz are the calibration signal.

electron aurora and H_β proton aurora (HIRASAWA and YAMAGISHI, 1980). When the rocket noise cone opened, it was in an intense break-up type aurora of about 40 k*R*. The auroral arc moved toward the geomagnetic south direction during the flight time (Fig. 3). At 57 s flight time, the receiver began to observe the noise and to measure the electron current in the aurora. The rocket emerged from the aurora at about 110 s and an altitude of 150 km. The measured direct electron current at an altitude of about 100 km was about five times larger during the ascent than that during the descent.

Figure 4 shows typical raw data of the AC component at various flight times, representing the emissions observed in the HF range. The noise level at 181.7 s and 330.5 s which increases slightly at the lower frequencies is due to the receiver noise. The observed emissions in the intense aurora (panels on the left side in Fig. 4) can be divided into three types according to the frequency ranges and spectrum shape. 1) There is a broad band low level noise ($\simeq 5\ \mu$V at maximum). For example, it extends to 7.4 MHz at 65.6 s. The upper frequency limit of the broad band noise gradually decreases with increasing altitude. At about 90 s, the noise extends from 1.4 to 3.8 MHz. 2) There are many narrow band high level signals ($\leq 50\ \mu$V at maximum) between 1.2 and 7.0 MHz. 3) There are also narrow band emissions whose frequencies are below the electron gyrofrequency ($\simeq 1.2$ MHz) as are clearly seen at 61.2 and 65.6 s in Fig. 4. The frequencies and intensities of the narrow band signals are plotted in Fig. 5.

The right-side panels in Fig. 4 show emissions received after the rocket passed out of the intense aurora. The broad band noise (type 1) has disappeared. The narrow band emissions of 1.4 and 1.6 MHz are observed to remain, as do those of 6.75 and 7.0 MHz. The large signal at 5.1 MHz is the calibration signal.

To see changes of the frequency and level of the emissions during the whole flight, a frequency versus time diagram, *i.e.*, a dynamic spectrum is shown in Fig. 6.

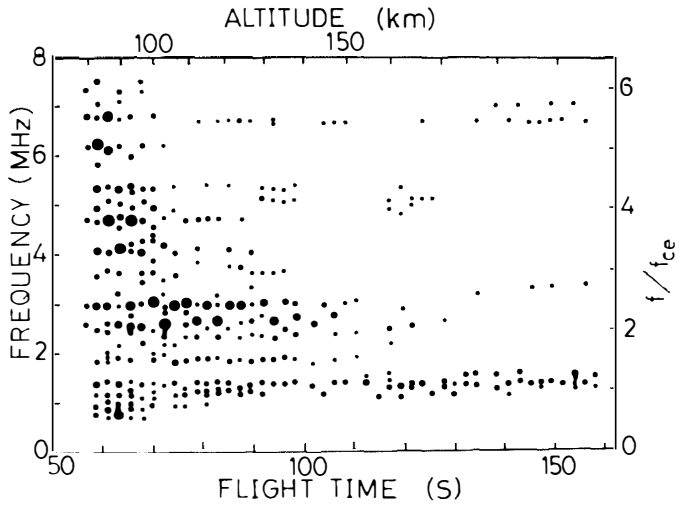

Fig. 5. Frequencies and intensities of the narrow band signals. Intensities are shown by the sizes of circles in seven steps. Harmonics of the electron cyclotron frequency are the values at the 100 km altitude.

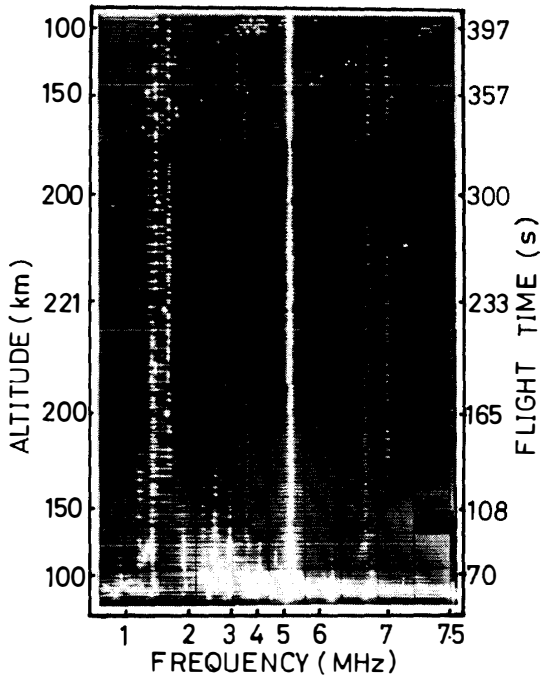

Fig. 6. Frequency versus time diagram. The noises observed during the whole flight are shown as white areas. The straight line at 5.1 MHz is the calibration signal.

It was made by photographing an intensity-modulated display on an oscilloscope. The white area shows the existence of signals observed by PWN-H. As mentioned above, three types of emissions are observed in the intense aurora up to approximately 110 s and below about 150 km on the ascent. In particular, type 2 signals are evident at the frequencies of 1.15, 1.35, 1.80, 2.25, 2.55, 2.95, 3.60, 4.00, 4.60, 6.15 and 6.75 MHz. The signal at 5.25 MHz merges with the calibration signal (5.1 MHz), however, it is clearly seen at 65.6 s in Fig. 4. After the rocket emerged from the aurora, signals at 1.4 and 1.6 MHz at a modest level ($\simeq 5\ \mu$V) continued to be observed. Signals at 3.5, 6.7 and 7.0 MHz were also detected at a 1 μV level. After about 100 s flight time, emissions at frequencies $1.4 \sim 1.7$ MHz, composed of some narrow band signals were received.

4. Discussions of the Results

As they were observed during the whole flight time at a constant frequency, the signals at 6.7 and 7.0 MHz are considered to be broad-casting waves from ground stations as were observed by MIYAOKA *et al.* (1981). As the sharp peaks at 1.4, 1.6, 3.2 and 3.5 MHz are observed in the quiet region above about 170 km, they would also seem to be broadcasting waves.

4.1. Type 1 emission

The frequency of the broad noise (type 1) decreases with the time of flight when the rocket is in the aurora, as seen in the left panels of Fig. 4. The upper-limiting frequency, f_{UL}, of the noise is thought as a characteristic frequency such as f_{pe}, $f_{L=0}$ or f_{UHR}. Here f_{pe}, $f_{L=0}$ and f_{UHR} are the electron plasma frequency, the L-mode cut-off frequency and the upper hybrid frequency, respectively. According to relations

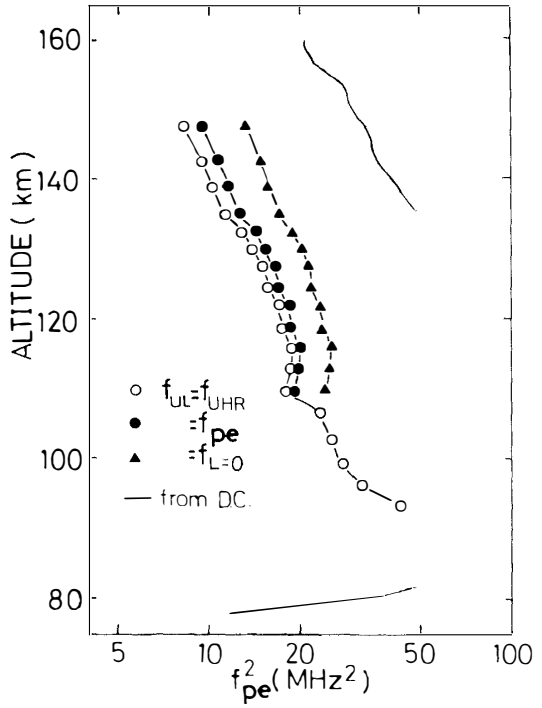

Fig. 7. f^2_{pe}, estimated from f_{UL} and DC to the grid, as a function of altitude.

$2f_{L=0}=(4f^2_{pe}+f^2_{ce})^{1/2}-f_{ce}$ and $f_{UHR}=(f^2_{pe}+f^2_{ce})^{1/2}$, a variety of values of f_{pe} can be estimated when f_{UL} is assumed to be equal to one of the characteristic frequencies. The electron cyclotron frequency f_{ce} has been calculated by using the IGRF 1975 model. The result is shown in Fig. 7. The open circles, closed triangles and closed circles correspond to f^2_{pe} for the cases where f_{UL} is equal to f_{UHR}, $f_{L=0}$ and f_{pe}, respectively. The solid line shows f^2_{pe} calculated from the electron density obtained by the *in situ* DC data. The current saturated between 82 and 136 km in which range the electron density is larger than 6×10^5 cm^{-3} when an electron temperature of 0.5 eV is assumed. Above the altitude of 145 km type 1 noise was not detected because the rocket had emerged from the aurora. At altitudes lower than 94 km, f_{UL} was above the upper sweep frequency limit (7.6 MHz) of the present instrument, as can be seen, for example, at 61.2 s in Fig. 4. Although the calculated density from the noise is about one third of the estimated density from the current, the trend of f^2_{pe} obtained, especially from that for $f_{UL}=f_{UHR}$, agrees with the current profile. The quantitative disagreement is assumed to be due to the error in evaluating the density from the current for the constant bias or that the emission is excited at a higher, lower-density altitude. Therefore, the broad band noise is considered to be the electron plasma or the upper hybrid wave. Emissions whose frequency is around f_{pe} have been received by previous rocket experiments (KELLOGG *et al.*, 1978; OYA *et al.*, 1980; MIYAOKA *et al.*, 1981). Since simultaneous measurement of the velocity distribution of electrons was not made, the mode of this emission can not be identified. However, when the distribution of precipitating electrons is monochromatic as was measured in an active aurora by ARNOLDY *et al.* (1974), the electron plasma wave becomes unstable (Cerenkov effect). Another possibility is that the electrostatic wave near f_{UHR} is destabilized when the electron distribution has a region of positive slope with respect to the perpendicular velocity (KURTH

et al., 1979, 1980).

The level of the type 1 noise at frequencies lying near the large narrow band emissions appears to be suppressed as is seen in the left panels in Fig. 4. Such phenomena were also observed for natural VLF emissions which were influenced by the Siple signal (KIMURA, 1981) and for electron plasma waves excited by an electron beam, which are suppressed by an externally launched signal, in a laboratory experiment (NAKAMURA, 1970).

It is noted that the lower-limiting frequency of the broad band noise seems to be constant, *i.e.*, about 1.4 MHz which is approximately equal to f_{ce}.

The frequency spectrum of the broad band emissions shows a temporal variation of the order of 0.1 s as seen in spectra at 61.2 and 65.6 s in Fig. 4. It is thought not to be spatial variation since the rocket velocity perpendicular to the geomagnetic field line is about 300 m/s. This type of noise is thought to be the same bursts as received by KELLOGG and MONSON (1979), which are emitted from an intense aurora.

4.2. Type 2 emission

Normalized frequencies of narrow band emissions, for example, observed at 100 km with f_{ce} (=1.226 MHz) are 0.94, 1.10, 1.47, 1.84, 2.08, 2.41, 2.94, 3.26, 3.84, 4.28, 5.01 and 5.51. Therefore, the type 2 emissions enter into the category of either nf_{ce} or $(n+1/2)f_{ce}$, where n is an integer. As seen in Figs. 5 and 6, the type 2 emissions appear to have an upper-limiting frequency which varies with the flight time. The upper-limiting frequency approximately agrees with f_{UL} of the type 1 broad noise described above. Emissions of larger amplitude exist at frequencies near f_{UL} and decrease in frequency when the density decreases, as is clearly seen in Fig. 5. For example, the emissions of 2.95 MHz ($\simeq 2.5\, f_{ce}$) at 76.5 s and 6.75 MHz ($\simeq 5.5\, f_{ce}$) at 56.8 s in Fig. 4 are in the type 1 broad band noise. The signals (1.4 to 1.7 MHz) which were lower than f_{pe} and which were received after passing out of the intense aurora seem to be f_{ce} or $(3/2)f_{ce}$ emissions.

Odd half-harmonic emissions $(n+1/2)f_{ce}$ for only $n=1$ have been observed in the aurora by KELLOGG *et al.* (1978). In the present experiment, the emissions up to $n=5$ have been observed together with the emissions related to f_{pe} or f_{UHR}. The behavior of $(n+1/2)f_{ce}$ emissions, that is, the intense emission appearing when $(n+1/2)f_{ce} \simeq f_{pe}$ or f_{UHR}, is similar to those observed in the outer magnetosphere (SHAW and GURNETT, 1975) and in the region just outside the plasma-pause (KURTH *et al.*, 1979; GURNETT *et al.*, 1979). The odd half-harmonic emissions $(n+1/2)f_{ce}$ which are smaller than f_{UHR} have been also excited by electron beams in laboratory experiments (IDEHARA *et al.*, 1969; BERNSTEIN *et al.*, 1975). Therefore, $(n+1/2)f_{ce}$ emissions are considered to be electron Bernstein modes. The modes become unstable when the distribution function of electrons has a region of positive slope with respect to the perpendicular velocity like the loss cone distribution, according to the theoretical studies (ASHOUR-ABDALLA and KENNEL, 1978; HUBBARD and BIRMINGHAM, 1978). However, the theory does not explain the coexistence of nf_{ce} and $(n+1/2)f_{ce}$ emissions as observed by this rocket. When precipitating electrons are monochromatic with a pitch angle of about zero and are considered to be a beam, one branch of the obliquely propagating cycrotron harmonic waves become unstable at two wavenumbers, that

is, at two frequencies between nf_{ce} and $(n+1)f_{ce}$ for a given n, due to Cerenkov and anomalous effects of the beam (SEIDL, 1970). IDEHARA *et al.* (1969) have observed nf_{ce} and $(n+1/2)f_{ce}$ emissions simultaneously when $f_{pe} \gg f_{ce}$ in the electron beam and plasma system.

The spectral width of the type 2 emissions is narrower than the band width of the receiver. Such a narrow band signal which is identified as the Bernstein mode has been observed KELLOGG *et al.* (1978). They consider it to be a natural emission since its frequency has shifted. In our case, except for three signals in Fig. 6 which are described below, the frequencies of type 2 emissions are rather constant. Due to the constancy of the frequencies and the narrow band, they are thought to originate from broadcasting radio waves from ground stations. The radio waves might excite electrostatic waves at an auroral boundary or might linearly converge to cyclotron harmonic waves at the density gradient which forms at north and south boundaries of the auroral arc. Then the electrostatic waves are amplified by the instabilities stated above. The three signals whose frequencies have shifted are around 1.3 MHz at 115 km, 3.5 MHz at 120 km and 6.7 MHz at 120 km as seen in Fig. 6. However, their frequencies seem to shift not continuously but discontinuously since frequencies of radio waves transmitted from many radio stations are so closely distributed.

4.3. Type 3 emission

The type 3 emission whose frequency lies below the gyrofrequency (1.2 MHz) is likely to be the whistler wave which has been observed by KELLOGG *et al.* (1978). The whistler wave which propagates near the resonance cone can strongly couple with precipitating electrons when $f_{ce} \ll f_{pe}$. As is clearly seen for the flight times 61.2 and 65.6 s in Fig. 4, the emission coexists with the intense burst-like noise which is thought to be the electron plasma oscillation or the upper hybrid wave. The coexistence of the whistler wave and the electron plasma wave has been studied experimentally in an electron-beam and plasma system in a laboratory (STENZEL, 1977). Such correlation of whistler waves and electron plasma oscillation bursts has recently detected in the solar wind (KENNEL *et al.*, 1980).

5. Conclusion

Observation of the following three types of emissions has been made in an intense aurora by PWN-H on board the sounding rocket S-310JA-7.

1) A broad band, low level, burst-like emission whose upper-limiting frequency is correlated with f_{pe} or f_{UHR} and whose lower-limiting frequency is nearly constant at 1.4 MHz which is approximately equal to f_{ce}.

2) Narrow band, high level emissions whose frequencies are nearly equal to nf_{ce} or $(n+1/2)f_{ce}$.

3) Whistler waves.

The whistler waves are correlated with the burst-like emission. Simultaneous generation of nf_{ce} and $(n+1/2)f_{ce}$ emissions with n as large as five has been observed for the first time by the present experiment. However, the generation mechanism of these emissions is uncertain since the velocity distribution function of electrons was

not measured. Therefore, simultaneous measurements of emissions and the velocity distribution of electrons parallel and perpendicular to the geomagnetic field should be performed in the future.

Acknowledgments

The authors would like to thank Prof. T. NAGATA, Director of the National Institute of Polar Research for providing the opportunity for the rocket experiment. They also thank Prof. T. HIRASAWA and Dr. H. YAMAGISHI for the data of the ground observations at Syowa Station.

References

ARNOLDY, R. L., LEWIS, P. B. and ISAACSON, P. O. (1974): Field-aligned auroral electron fluxes. J. Geophys. Res., **79**, 4208–4221.

ASHOUR-ABDALLA, M. and KENNEL, C. F. (1978): Nonconvective and convective electron cyclotron harmonic instabilities. J. Geophys. Res., **83**, 1531–1543.

BERNSTEIN, W., LEINBACH, H., COHEN, H., WILSON, P. S., DAVIS, T. N., HALLINAN, T., BAKER, B., MARTZ, J., ZEIMKE, R. and HUBER, W. (1975): Laboratory observations of *RF* emission at ω_{pe} and $(n+1/2)\omega_{ce}$ in electron beam-plasma and beam-beam interactions. J. Geophys. Res., **80**, 4375–4379.

GURNETT, D. A., ANDERSON, R. R., SCARF, F. L., FREDRICKS, R. W. and SMITH, E. J., (1979): Initial results from ISEE-1 and -2 plasma wave investigation. Space Sci. Rev., **23**, 103–122.

HIRASAWA, T. and YAMAGISHI, H. (1980): Electron number density within auroras. Highlights of the Japanese IMS program, I.S.A.S., 27–33.

HUBBARD, R. F. and BIRMINGHAM, T. J. (1978): Electrostatic emissions between electron gyroharmonics in the outer magnetosphere. J. Geophys. Res., **83**, 4837–4850.

IDEHARA, T., OHKUBO, K. and TANAKA, S. (1969): Instability near electron cyclotron harmonic frequencies in beam-beam system. J. Phys. Soc. Jpn., **27**, 187–197.

ITOH, T., NAKAMURA, M. and NAKAMURA, Y. (1975): Rocket observation of electron density irregularities in the middle latitude *E* region. Geophys. Res. Lett., **2**, 553–555.

KELLOGG, P. J., MONSON, S. J. and WHALEN, B. A. (1978): Rocket observation of high frequency waves over a strong aurora. Geophys. Res. Lett., **5**, 47–50.

KELLOGG, P. J. and MONSON, S. J. (1979): Radio emissions from the aurora. Geophys. Res. Lett., **6**, 297–300.

KENNEL, C. F., SCARF, F. L., CORONITI, F. V., FREDRICKS, R. W., GURNETT, D. A. and SMITH, E. J. (1980): Correlated whistler and electron plasma oscillation bursts detected on ISEE-3. Geophys. Res. Lett., **7**, 129–132.

KIMURA, I. (1981): VLF wave-particle correlation observed by EXOS-B satellite. US-Japan Seminar on Wave-particle Interactions in Space Plasmas, 10–14.

KURTH, W. S., CRAVEN, J. D., FRANK, L. A. and GURNETT, D. A. (1979): Intense electrostatic waves near the upper hybrid resonance frequency. J. Geophys. Res., **84**, 4145–4164.

KURTH, W. S., FRANK, L. A., ASHOUR-ABDALLA, M., GURNETT, D. A. and BUREK, B. G. (1980): Observations of a free-energy source for intense electrostatic waves. Geophys. Res. Lett., **7**, 293–296.

MIYAOKA, H., OYA, H. and MIYATAKE, S. (1981): Observations of MF-HF plasma wave emissions in the polar ionosphere using the Antarctic rockets S-310JA-4 and S-310JA-6. Mem. Natl Inst. Polar Res., Spec. Issue, **18**, 462–490.

NAKAMURA, Y. (1970): Suppression of two-stream instability by beam modulation. J. Phys. Soc. Jpn., **28**, 1315–1321.

OYA, H., MIYAOKA, H. and MIYATAKE, S. (1979): Nankyoku roketto S-310JA-1, 2-gôki ni yoru kôshûha-

tai denpa hôsha no kansoku-PWH no kansoku kekka (Observation of HF plasma wave emissions at ionospheric level using sounding rockets S-310JA-1, 2, in Antarctica). Nankyoku Shiryô (Antarct. Rec.), **64**, 30–41.

OYA, H., MIYAOKA, H. and MIYATAKE, S. (1980): Nankyoku roketto S-210JA-21-gôki ni yoru kôshûha purazuma hadô supekutoru no kansoku (Observation of HF plasma wave spectrum at ionospheric level using sounding rocket S-210JA-21 in Antarctica). Nankyoku Shiryô (Antarct. Rec.), **69**, 37–51.

SEIDL, M. (1970): Temperature effects on high-frequency beam plasma interaction. Phys. Fluids, **13**, 966–979.

SHAW, R. S. and GURNETT, D. A. (1975): Electrostatic noise bands associated with the electron gyrofrequency and plasma frequency in the outer magnetosphere. J. Geophys. Res., **80**, 4259–4271.

STENZEL, R. L. (1977): Observation of beam-generated VLF hiss in a large laboratory plasma. J. Geophys. Res., **82**, 4805–4814.

(*Received November 13, 1981; Revised manuscript received January 5, 1982*)